Fragmentation of Radical Anions of Polyfluorinated Benzoates

Valery V. Konovalov,*,†,‡ Sergey S. Laev,§ Irina V. Beregovaya,§ Lyudmila N. Shchegoleva,§ Vitalij D. Shteingarts,*,§ Yuri D. Tsvetkov,† and Itzhak Bilkis||

Institute of Chemical Kinetics and Combustion and Institute of Organic Chemistry, Siberian Branch of Russian Academy of Sciences, 630090, Novosibirsk, Russia, and The Hebrew University of Jerusalem, Faculty of Agriculture, PO Box 12, Rehovoth 76−100, Israel

Received: September 20, 1999

A comprehensive study of the symmetry forbidden fragmentation of short-lived radical anions (RAs) has been undertaken for the complete set of polyfluorinated benzoates ($C_6F_nH_{5-n}CO_2^-$, $n = 1-5$). The decay rate constants (k_c) of RAs have been determined in aqueous alkaline solution (pH 13.4) by electron photoinjection (EPI) from mercury electrodes and were found to increase dramatically from $\leq 3 \times 10^3$ s^{-1} (3-F−$C_6H_4CO_2^-$) to $(1.2 \pm 0.8) \times 10^9$ s^{-1} ($C_6F_5CO_2^-$). The regioselectivity of C−F bond cleavage in the RA fragmentation has been revealed by structure assignment of reduction products of the polyfluorinated benzoic acids by Na, K, and Zn in liquid NH_3, as well as by Zn in aqueous NH_3 and aqueous alkaline solutions. The k_c values depend on the position of the cleaved fluorine to the CO_2^- group generally in the order para > ortho > meta, and to sharply increase if adjacent fluorine atoms are present. The observed trends reveal that the kinetics of the RA fragmentation reaction is not controlled by the reaction thermodynamics. Semiempirical UHF/INDO calculations, the validity of which has been confirmed by ab initio ROHF/6-31+G calculations, were done to rationalize the observed trends. The reaction transition state (TS) was considered to arise from the RA's Π and Σ^* states crossing avoided due to out-of-plane deviation of the cleaving C−F bond. The satisfactory linear correlation ($R = 0.96$) between the model reaction energy barrier E_a and log k_c has been achieved with modeling the local solvation of the CO_2^- group by its protonation.

Introduction

One-electron reduction of haloarenes leads to the formation of metastable radical anions (RAs)[1,2] which are of major importance as intermediates in many conversions of these compounds.[3] Research in haloarene RAs provides results[1−5] that are of crucial significance for modern theory of RAs dealing with the relationships of their spatial structure, spectral characteristics, and reactivity.

Haloarene RAs ($ArX^{\bullet -}$) are known to decay in polar solvents, usually with formation of aryl radicals and halide ions (eq I).[1,2,6]

$$ArX^{\bullet -} \xrightarrow{k_c} Ar^{\bullet} + X^- \qquad \text{(I)}$$

For planar π-type $ArX^{\bullet -}$, monomolecular elimination of X^- is forbidden by symmetry since it results in the σ-type phenyl radical $Ar^{\bullet}$ and closed-shell halide ion.[7]

The decay rate constants (k_c) of RAs of monohaloarenes in aqueous solutions have been determined by pulse radiolysis[1] and in aprotic organic solvents by various direct and indirect electrochemical techniques.[2,3c−e,8−11] A dramatic change in RA lifetime by changes in the aryl moiety while the leaving group remained the same has been demonstrated.[12] Electrochemical studies showed that the k_c value parallels the standard reduction potential $E^0_{ArX/ArX^{\bullet -}}$ of the starting molecules;[2,3c−e,8−11] that is, the more negative the reduction potential, the faster the cleavage. In some cases, the role of bond dissociation energies D_{ArX} also became important. For RAs of fluoromethylarenes it was shown that the role of the D_{ArX} is much larger than that of $E^0_{ArX/ArX^{\bullet -}}$.[13]

Although a large number of monohaloarene compounds was investigated, the trends of polyhaloarene RA decomposition with multiple equivalent leaving groups were poorly studied. Among them, polyfluoroarene RAs are of particular interest. Specifically, reductive defluorination of polyfluoroarenes, believed to involve intermediate RA formation, is a promising route to partially fluorinated arenes which often are less accessible than precursors but potentially valuable starting materials for syntheses. Moreover, the electronic structure of polyfluoroarene RAs is of considerable theoretical interest because of the fact that fluorine accumulation can cause the RA to become a nonplanar pseudo-π-radical. Their SOMO contains an admixture of σ^* orbitals, the extent of which depends on the location and increases with the number of the fluorine atoms.[5] It has been shown that the trend of the polyfluoroarene RAs cleavage differs from what was known for simple halides. Despite the fact that fluoroarenes have reduction potentials $E^0_{ArX/ArX^{\bullet -}}$ generally more positive than those of nonfluorinated compounds,[3f,14] a dramatic decrease of RA stability has been observed with fluorine accumulaton,[14] instead of the increase expected from the theory of intramolecular dissociative electron transfer[15] linking the k_c values with the reaction driving force.[16] In this connection it should be noted that the bond dissociation free energy D_{ArX}, which contributes to the driving force, increases with the fluorine

* To whom correspondence should be addressed. Fax: (205) 348-2346; E-mail: vvk01@bama.ua.edu; shtein@nioch.nsc.ru.

† Institute of Chemical Kinetics and Combustion, Siberian Branch of Russian Academy of Sciences.

‡ Present address: Center for Materials for Information Technology (NSF MRSEC), The University of Alabama, P.O. Box 870209, Room 205 Bevill Building, Tuscaloosa, AL 35487.

§ Institute of Organic Chemistry, Siberian Branch of Russian Academy of Sciences.

|| The Hebrew University.

10.1021/jp993361d CCC: $19.00 © 2000 American Chemical Society
Published on Web 12/04/1999

accumulation. For example, D_{ArX} are 117 and 145 kcal/mol in fluorobenzene and hexafluorobenzene, respectively.[17] Thus, preliminary results indicate that with polyfluoroarene RAs we have a situation where the kinetics of cleavage reaction is not controlled by its thermodynamics; that is, the reaction intrinsic barrier is not controlled by the reaction driving force. A comprehensive study of the effect of fluorine accumulation and location on the kinetics and regioselectivity of RA fragmentation is necessary to determine the factors governing fluoroarene reductive activation and its relation to the molecular structure.

In the gas phase, the cleavage of fluoroarene RA does not occur[18] but becomes possible in a polar solvent primarily due to the solvation of the incipient fluoride ion.[19] This fact makes some difficulties for direct quantum chemical investigation of the process, since an appropriate taking into account of solvation is necessary to locate the reaction transition state (TS). An alternative way is the TS modeling. Such a theoretical approach concerning the symmetry-forbidden fragmentation of polyfluorobenzene RAs with the elimination of F^- has been proposed recently.[19,20]

Pulse radiolysis and conventional electrochemistry have a number of limitations for the study of short-lived RAs. The time resolution of pulse radiolysis allows the determination of $k_c < 10^7-10^8$ s^{-1},[1,21] and of electrochemistry up to 10^7 s^{-1} with ultramicroelectrodes,[9] and up to 10^9 s^{-1} by using a redox-catalysis process.[2] Electron photoinjection (EPI) from metal electrodes[22-26] can produce solvated electrons in close electrode vicinity in a wide range of cathodic potentials.[27] The high reducing power of solvated electrons[28] makes RA generation possible at an electrode potential which may be much more positive than the reduction potential of the starting electron scavengers. Thus, EPI complements the traditional (dark) electrochemical methods.[26] Another advantage of EPI for the study of short-lived RAs is the absence of diffusion limitations due to the very short distance between photoproduced solvated electrons and the electrode (5−60 Å).[24] This permits the determination of k_c of reduced transients in the range of $3 \times 10^3-10^9$ s^{-1}.[4,25] Decay rate constants of RAs of monohalogenated benzoates[4a] and aryltrimethylammonium salts[25] have been obtained.

This paper presents the results of a systematic investigation of the RA fragmentation of the full set of fluorinated benzoates. The decay rate constants of RAs were measured by the EPI technique. Most of the calculations were performed by the INDO method, which has been shown to be the only semiempirical method correctly predicting the electronic and spatial structure as well as the reactivity of polyfluorobenzene RAs.[20,29a] General trends of fluoroarene RA fragmentation related to the RA structure are revealed and the applicability of the EPI technique to the transient intermediates research is advanced.[30]

Experimental Section

Materials. For EPI experiments aqueous solutions of KCl (0.5 M) and KOH (pH 13.4) at 20−22 °C were used. Water was purified by four-fold distillation in a quartz vessel with γ-ray and UV irradiation. KCl was "superpure" grade, and mercury was "ROD". The concentration of uncontrolled impurities was less than 10^{-5} M (in terms of N_2O reactivity with e^-_{aq}). N_2O, used as a reference electron scavenger, was "pure" grade.

Acids **1**, **3**, and **18** were commercially available. Compound **2**, mp[31] 121−122 °C (lit.[32] 122−124 °C), was prepared by reaction of 3-fluorobenzoyl chloride with water. Acids **4**, **7**, **11**, **13**, and **16** were synthesized by reaction of 1,2-difluoro-, 1,3-difluoro-, 1,2,4-trifluoro-,[33] 1,3,5-trifluoro-, and 1,2,3,5-tetrafluorobenzene, respectively, with butyllithium in THF at −70 °C, followed by carboxylation,[34] mp 160−162, 158−160, 128−129, 145−147, and 97−99 °C (lit.[32,35] 163−165, 158−160, 130−131, 142−145, and 98−99.5 °C). Acetylation by AcCl of *meta*-, *para*-, and *ortho*-difluorobenzenes and 1,2,4-trifluorobenzene[36] followed by oxidation of the resulting acetophenones by potassium permanganate[37] gave **5**, **6**, **8**, and **12**, mp 184−186, 132−133, 123.5−125, 97.5−99 °C (lit.[32] 188−190, 132−134, 122−124, 99−101 °C). Acids **9** (mp 119.5−120.5 °C, lit.[32] 121−123 °C) and **14** (mp 98−99.5 °C, lit.[32] 97−99 °C) were synthesized from 3,5-difluoroaniline[38] and 3,4,5-trifluoroaniline,[38] respectively, via substitution of the amino group by bromine using the Sandmeyer reaction followed by carboxylation[39] of the Grignard reagents prepared from the resulting 3,5-difluoro- and 3,4,5-trifluorobromobenzene. Compound **10** was obtained from α,α,α,2,3,5,6-heptafluorotoluene by reaction with hydrazine hydrate in ethanol, followed by oxidation of α,α,α,2,3,5-hexafluoro-*o*-tolylhydrazine by copper(II) sulfate and hydrolysis of the trifluoromethyl group analogous to the procedure of ref 40, mp 107−108 °C (lit.[41] 106 °C). Acid **15** (mp 89−90 °C, lit.[32] 85−87 °C) was obtained by decarboxylation of tetrafluorophthalic acid;[42] acid **17** (mp 149−151 °C, lit.[32] 150−152 °C) was synthesized by hydrodefluorination of **18**.[43] Compound **19** (mp 138.5−140 °C, lit.[32] 140−142 °C) was prepared from 3,4,5-trifluoroaniline by replacement of the amino group by hydrogen[44] followed by the reaction of 1,2,3-trifluorobenzene with butyllithium in THF and carboxylation.[39]

EPI Measurements. The pulsed laser photoelectrochemical setup described in detail earlier[23-24] was used. The measurements were performed using a three-electrode cell with a replaceable-fixed mercury electrode[22d] and a saturated calomel electrode as reference. The light source was a homemade pulsed excimer laser at 351 nm (XeF). Control measurements were also carried out at 308 (XeCl), 337 (N_2 laser), and 427 nm (N_2^+ laser). At all laser wavelengths, the absorbance of the solution phase species was negligible. The light path in solution was 0.1−0.2 mm, the compound concentrations varied from 10^{-4} to 10^{-1} M, and the extinction coefficient of all compounds at these wavelengths was less than 2 mol^{-1} cm^{-1}.

The experimental value of the electrode photopotential $U(t)$ was no more than 1−2 mV. The photoinduced charge Q was calculated from the area under the exponential RC-decay of $U(t)$ which is realized at fairly long times ($t > 50$ μs) after the laser pulse.[23a] The RC-decay constant (about 300−500 μs) was calculated together with Q. The photopotential was measured beginning at $t = 50$ μs when all photodiffusion processes are over and there is no additional heating photosignal. The differential capacity of electrical double layer was controlled by the RC-decay constant and use of a conventional RCL-bridge. The measurement error for the photoinduced charge was ±3%.

Reduction of Polyfluorobenzoic Acids by Metals. *i. Alkali Metals in Liquid NH_3.* Since for acid **18**, as an example, various orders of reagent mixing (addition of the acid to a metal solution in liquid NH_3, addition of alkaline metal pieces or drops of metal solution in liquid NH_3 to an ammonium benzoate solution) and the variation of metal identity (Na or K) gave the same results, the remaining acids were reduced by the following procedure. A polyfluorobenzoic acid (2−4 mmol) and Na or K (6−12 mmol) were added sequentially to stirred liquid NH_3 (50−70 mL, distilled from Na) at −45 °C. After 15 min, water (5 mL) and ether (20 mL) were added and volatiles were removed under reduced pressure. The residue was treated with aq HCl and extracted with ether. The extracts were combined and dried over $MgSO_4$ and ether was evaporated. The residue (yield 70−85%)

was analyzed by ^{1}H and ^{19}F NMR spectroscopy in CD_3COCD_3 using a Bruker WP-200 SY spectrometer at 200.1 and 188.3 MHz, respectively**.** The following mole product distribution was found. From **4** (the ratio of acid to sodium was 1:1.5): **2** (7%), **20** (2%), unidentified compounds (un.c.) (26%), and starting material (s.m.) (65%). From **6**: **2** (40%), **20** (10%), un.c. (45%), and s.m. (5%). From **8**: **2** (55%), **20** (20%), un.c. (7%), and s.m. (18%). From **11**: **2** (9%), **6** (16%), **20** (9%), un.c. (26%), and s.m. (40%). From **16**: **2** (16%), **11** (12%), **20** (9%), un.c. (8%), and s.m. (≥55%). From **17**: **2** (14%), **9** (5%), **20** (7%), un.c. (5%), and s.m. (70%). From **18**:[60] **2** (10%), **9** (3%), **17** (≤8%), **20** (≤4%), un.c. (<20%), and s.m. (≥60%). From **19**: **2** (13%), **4** (18%), **5** (<2%), **8** (3%), **20** (20%), un.c. (7%), and s.m. (37%). The major portion of unidentified compounds consisted of cyclohexadiene derivatives as shown by the signals of olefinic protons in the ^{1}H NMR spectra (δ 6.30−6.75 ppm). The unidentified products were probably derived from **2** since they were also obtained by reduction of this acid under the same conditions.

ii. Zn in Liquid NH_3. A polyfluorobenzoic acid (2−3 mmol) was added to active Zn powder, produced by reduction of $ZnCl_2$ with Na (6−9 mmol) in liquid NH_3 (50−60 mL), and the mixture was stirred at −45 °C for 3.5−4.5 h. Product isolation, as described in section *i*, gave a residue (≥85%) which was analyzed by ^{1}H and ^{19}F NMR spectroscopy. The following mole product distribution was found. From **14**: **9** (17%) and s.m. (83%). From **15**: **10** (30%) and s.m. (70%). From **16**: **11** (9%), **12** (11%), and s.m. (80%). From **18**:[60] **17** (100%).

iii. Zn in Aqueous NH_3.[45] Acid **15** or **18** (4 mmol), Zn powder (20 mmol), and ∼20% aqueous NH_3 (20 mL) were stirred at room temperature for 29 or 5 h. Unreacted Zn was separated and washed with water. The aqueous solution was acidified with HCl and extracted with ether (3 × 30 mL). The combined ethereal extracts were dried over $MgSO_4$. The solvent was removed under reduced pressure to yield respectively a mixture of **10** (83%) and s.m. (17%) or **17** as the sole product (92%).

iv. Zn in Aqueous Alkali. A mixture of **18** (4 mmol), Zn powder (24 mmol), and an aqueous solution (20 mL) of NaOH or KOH (20 mmol) and H_2O (20 mL) was stirred in water at 60 °C for 20 h. Analogous isolation (section iii) gave a mixture containing **17** (60%), 4-hydroxy-2,3,5,6-tetrafluorobenzoic acid (20%), and s.m. (20%).

Quantum Chemical Calculations. Most calculations were performed by the UHF/INDO method which, unlike MNDO-type methods, results in an adequate description of the electronic and geometric structures of polyfluoroaromatic RAs.[20] Some additional ab initio ROHF/6-31+G calculations using the GAMESS program[46] were made to check the validity of INDO results for benzoate and benzoic acid RAs. Geometry optimization was carried out for all benzoate RAs and their protonated forms (RAs of the corresponding benzoic acids). For each RA, the energy of excited states was calculated by using the optimized ground-state geometry of the RA planar structure. The self-consistent Hartree−Fock solutions for RA excited states were found by changing the guess density matrix in combination with the level shift technique,[47] the convergence accuracy being no worth than 10^{-5} au. Potential curves for F^- elimination were obtained at a frozen ring geometry optimum for a planar structure of the initial RA. For model TS, a geometry was optimized completely, fixing the distance C−F as a single parameter, corresponding to concrete models. The modified PC version of the SPINHAMILTONIAN program was used.[47] In addition, some single-point calculations using the solvaton model,[48] realized within the INDO scheme, were performed to estimate nonspecific solvation effects. The Molden package was used to produce the SOMO plots.[49]

Results and Discussion

Fragmentation Rate Constants (k_c). The sequence of bulk and electrode reactions induced by photoinjected electrons in a solution containing scavenger ArX can be written as follows:[24d]

$$e^-_{met} + \text{light} \underset{\xi e(Q_e)}{\overset{(Q_o)}{\rightleftharpoons}} e^-_{aq} \tag{1}$$

$$e^-_{aq} + ArX \xrightarrow{k_a(Q_a)} ArX^{\bullet -} \tag{2}$$

$$ArX^{\bullet -} \xrightarrow{\xi_a(Q_1)} ArX + e^-_{met} \tag{3}$$

$$ArX^{\bullet -} \xrightarrow{k_c(Q_2)} Ar^\bullet + X^- \tag{4}$$

$$Ar^\bullet + \nu e^-_{met} \rightarrow P \tag{5}$$

where e^-_{met} is the metal electron, k_e is the rate constant of the reaction of e^-_{aq} with scavenger ArX, and ξ_e and ξ_a are the rate constants of electrode reaction of e^-_{aq} and $ArX^{\bullet -}$. The photoinduced charge Q passing from metal into solution for eq 1−5 is of the form

$$Q = Q_o - Q_e - Q_1 + \nu(E)Q_2 = (1 + \nu(E))Q_2 = \begin{cases} 2Q_2, \nu = 1 \\ Q_2, \nu = 0 \\ 0, \nu = -1 \end{cases} \tag{6}$$

$$Q_a = Q_o - Q_e = Q_1 + Q_2 \tag{7}$$

where $Q_o(E) = A(E_{thr} - E)^{5/2}$ [22b−e,23c] is the full photoinjected charge; Q_e is the charge of e^-_{aq} returned to the electrode; Q_a is the accepted charge; Q_1 and Q_2 are the charges of the $ArX^{\bullet -}$ oxidation and conversion into $Ar^\bullet$; $\nu(E)$ tends to ±1 for one-electron reduction or oxidation of $Ar^\bullet$. Thus, complete reduction of $Ar^\bullet$ doubles the charge Q_a and oxidation of all phototransients leads to zero photocharge. The dependence $Q/Q_2 = 1 + \nu(E)$ represents a photopolarogram of the decay product $Ar^\bullet$.[26] The charge Q can be calculated from the diffusion equations for e^-_{aq}, $ArX^{\bullet -}$ and $Ar^\bullet$ by the operator method:

$$\frac{Q}{2Q_o} = 1 - \frac{\tilde{f}(l_e^{-1})}{1 + l_s/l_e} - \frac{1 + l_s/l_a}{1 + l_{ox}/l_a}\frac{\tilde{f}(l_e^{-1}) - \tilde{f}(l_a^{-1})}{(l_e/l_a)^2 - 1} \tag{8}$$

where $\tilde{f}(l^{-1}) = \int_0^\infty f(x)e^{-x/l}\,dx$, $f(x)$ is the initial distance distribution function for e^-_{aq} normalized to unity, $l_e = (D_e/k_aC^o)^{1/2}$ and $l_a = (D_a/k_c)^{1/2}$ are the diffusion lengths of e^-_{aq} and $ArX^{\bullet -}$, C^o is the scavenger concentration; D_e and D_a are the diffusion coefficients of e^-_{aq} and $ArX^{\bullet -}$, $l_s = D_e/\xi_e$, and $l_{ox} = D_a/\xi_a$. For high and low scavenger concentrations asymptotic expressions are valid ($x_1 = \int_0^\infty f(x)x\,dx$):

$$\frac{Q(C^o)}{2Q_o} = \begin{cases} (x_1 + l_s)/l_e + ..., & x_1 \ll l_e \\ 1 - \dfrac{1 + l_s/l_a}{1 + l_{ox}/l_a}\tilde{f}(l_a^{-1}), & x_1 \gg l_e \end{cases} \tag{9}$$

Thus, with very fast RA decay ($k_c^{-1} = 0$) at the limit of high concentration the double photoinjected charge $2Q_o$ is attained, and a k_c-dependent limiting charge $Q_{lim} = Q(C^o \rightarrow \infty)$ less than $2Q_o$ is attained in the case of finite lifetime of RA. The charge asymptote at low concentration is independent of the type of

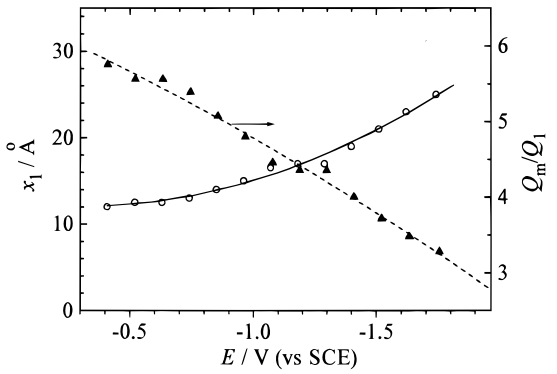

Figure 1. Dependence of $Q_m(E)/Q_1(E)$ and $x_1(E)$ on electrode potential E for 0.5 M KCl aqueous electrolyte solution obtained with N_2O.

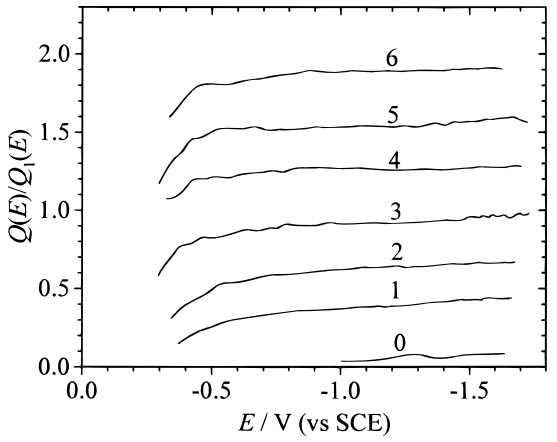

Figure 2. Dependence of photoinduced charge $Q(E,C^o)/Q_1(E)$ on electrode potential E in aqueous solutions of **18′** at different concentrations C^o: (0) background, (1) 1.12 mM, (2) 3.26 mM, (3) 8.4 mM, (4) 17.4 mM, (5) 32 mM, (6) 52 mM.

initial function $f(x)$ and the cleavage rate k_c. For very slow cleavage ($x_1 \ll l_a$), $Q_{lim} = x_1/l_a$ and thus does not depend on the type of $f(x)$. According to analysis,[23c,24a] in aqueous solutions a set of possible functions $f(x)$ lies between $\delta(x - x_1)$ and $1/x_1 \exp(-x/x_1)$, although the former was considered to be preferable. To calculate k_c we used both of these functions.

The first possibility to obtain k_c is by fitting the $Q(C^o)$ dependence according to eq 8, which requires knowledge of the type of $f(x)$ function and absolute values of all parameters. The second possibility is based on using a reference scavenger whose RA has a very short lifetime, e.g., N_2O ($k_c > 5 \times 10^9$ s^{-1}).[24a] In this case $Q_m = 2Q_o$ and x_1 (Figure 1) can be measured independently[24] and then applied to the asymptotic Q_{lim} charge in eq 9. Thus, it is sufficient to carry out measurements for only high scavenger concentrations and it is unnecessary to know k_a. For a mercury electrode and aqueous solutions the rate of e^-_{aq} decay at the electrode is very high[28] and therefore $l_s \approx 0$.[24a] The rate of RA oxidation on the electrode is estimated as high at potentials ($E \leq -1.6$ V) much more positive than the reduction potential of benzoates and it can be assumed that $l_{ox} \approx 0$.

Alkaline aqueous solutions (pH 13.4) were chosen for EPI measurements to provide the high concentration of benzoates (up to 10^{-1} M) that is required for correct extraction of k_c from the EPI data. This also precluded protonation of the RAs.[50a]

To use eq 8 one should initially obtain the photopolarograms $Q(E)/Q_1(E)$ (Figure 2) and determine the range of electrode potentials in which the RA decay products are electrochemically reduced, which corresponds to the climb of $Q(E)/Q_1(E)$ to the plateau. Initially electrolyte solution was saturated with N_2O and the dependence of $Q_1(E)$ was measured; subsequently, argon was bubbled through the solution to remove N_2O and polyfluorobenzoic acid was added.

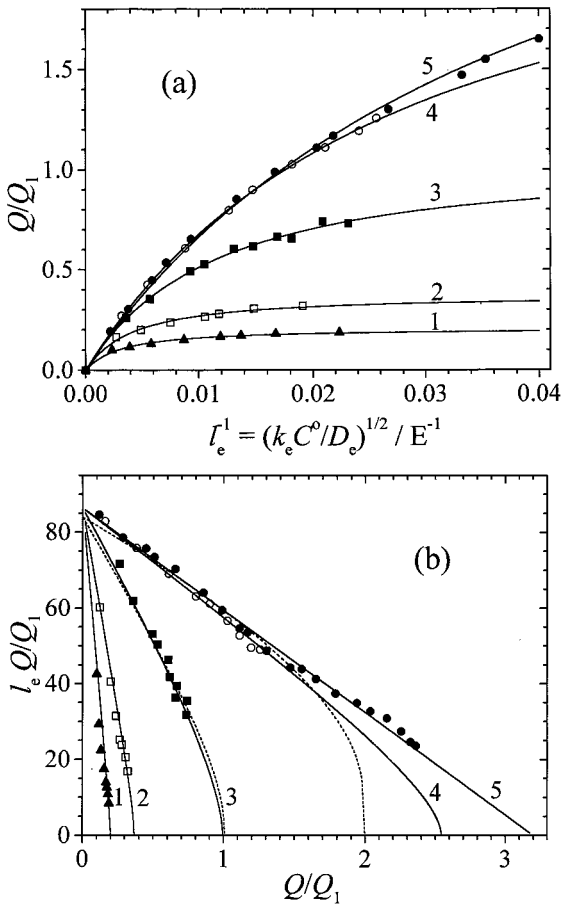

Figure 3. (a) Dependence Q/Q_1 (l_e^{-1}) for different fluorobenzoates at $E = -1.6$ V (SCE); (1) **3′**, (2) **7′**, (3) **17′**, (4) **18′**, (5) N_2O. (b) Dependence l_eQ/Q_1 (Q/Q_1). Simulation of Q/Q_1 using eq 9: solid line using $f(x) = 1/x_1 \exp(-x/x_1)$, dotted line $\delta(x - x_1)$.

The concentration dependence $Q(C^o)/Q_1$ (Figure 3a) was measured at the potential $E = -1.6$ V (SCE) corresponding to the rise to the plateau in the photopolarograms of all fluorobenzoates. The results of simulation of $Q(C^o)/Q_1$ with eq 8 are shown in Figure 3b. The diffusion coefficient for all benzoates was taken as 9.1×10^{-6} cm^2 s^{-1}.[51]

The structures of the fluorinated benzoates (**1′**−**18′**), obtained from the corresponding acids (**1**−**18**), and the k_c values of their RAs are listed in Table 1. The value for **3′** is in fair agreement with that found by pulse radiolysis.[1c,53] The range of k_c of about 6 orders of magnitude shows the dramatic increase with fluorine accumulation. The k_c values also depend on the positions of the fluorine atoms. The k_c values of the isomeric monofluoro compounds depend on the position of the cleaved fluorine to the CO_2^- group in the order para > ortho > meta. The values obtained for difluoro compounds (**5′** > **7′** > **6′**; **8′** > **4′**; **6′** > **9′**) are in agreement with this conclusion. In addition to the fluorine location relative to the CO_2^- group, the orientation of fluorine atoms relative to each other has a significant effect on the fragmentation rate. Thus, the RA stability decreases substantially when the fluorine atoms occupy adjacent sites: **4′** > **7′** > **6′**; **8′** > **5′**; and **14′** > **12′** > **13′**. However, for some compounds the order of k_c values (**4′** ≫ **10′** and **11′** > **17′**) contradicts these trends and shows that an additional fluorine atom at the meta position stabilizes the RA.

TABLE 1: Rate Constants of the Reaction of e^-_{aq} with Fluorinated Benzoates (k_e) and Fragmentation Rate Constants (k_c) of Benzoate RAs

n′	compound	k_e ($mol^{-1}\,s^{-1}$)	$l_a^{(1)}$ [a] (Å)	$l_a^{(2)}$ [a] (Å)	k_c [b] (s^{-1})
1′	2-F-$C_6H_4CO_2$-	3.1×10^9 [c]	2500	2500	$(1.5 \pm 0.8) \times 10^4$
2′	3-F-$C_6H_4CO_2$-	6.7×10^9 [c]	≥5500	≥5500	$\leq 3 \times 10^3$
3′	4-F-$C_6H_4CO_2^-$	3.8×10^9 [c]	405	425	$(5 \pm 2) \times 10^5$
		2.7×10^9 [d]			$(2.3 \pm 0.5) \times 10^5$ [d]
					$(6 \pm 1) \times 10^5$ [e]
4′	2,3-$F_2-C_6H_3CO_2^-$	4.1×10^9 [d]	70	80	$(1.6 \pm 0.8) \times 10^7$
5′	2,4-$F_2-C_6H_3CO_2^-$	3.5×10^9 [d]	73	83	$(1.5 \pm 0.7) \times 10^7$
6′	2,5-$F_2-C_6H_3CO_2^-$	2.7×10^9 [d]	802	810	$(1.4 \pm 0.6) \times 10^5$
7′	2,6-$F_2-C_6H_3CO_2^-$		206	230	$(1.9 \pm 0.8) \times 10^6$
8′	3,4-$F_2-C_6H_3CO_2^-$		32	40	$(7 \pm 3) \times 10^7$
9′	3,5-$F_2-C_6H_3CO_2^-$		3000	3000	$(1 \pm 0.8) \times 10^4$
10′	2,3,5-$F_3-C_6H_2CO_2^-$		365	380	$(6.5 \pm 2.5) \times 10^5$
11′	2,3,6-$F_3-C_6H_2CO_2^-$		25	33	$(1.1 \pm 0.5) \times 10^8$
12′	2,4,5-$F_3-C_6H_2CO_2^-$		25	33	$(1.1 \pm 0.5) \times 10^8$
13′	2,4,6-$F_3-C_6H_2CO_2^-$		34	41	$(6.5 \pm 2.5) \times 10^7$
14′	3,4,5-$F_3-C_6H_2CO_2^-$	4.2×10^9 [d]	15	20	$(2.0 \pm 1.0) \times 10^8$
15′	2,3,4,5-$F_4-C_6HCO_2^-$	3.9×10^9 [d]			$(1.7 \pm 0.6) \times 10^8$
16′	2,3,4,6-$F_4-C_6HCO_2^-$		7	13	$(1.2 \pm 0.8) \times 10^9$
17′	2,3,5,6-$F_4-C_6HCO_2^-$		60	70	$(2.1 \pm 0.8) \times 10^7$
18′	$C_6F_5CO_2^-$	4.4×10^9 [d]	7	13	$(1.2 \pm 0.8) \times 10^9$

[a] $l_a^{(1)}$ was fitted with function $f(x) = 1/x_1 \exp(-x/x_1)$ and $l_a^{(2)}$ with $\delta(x - x_1)$. [b] k_c were taken as the mean value of those calculated from $l_a^{(1)}$ and $l_a^{(2)}$. [c] Reference 52. [d] Reference 53. [e] Reference 1c.

SCHEME 1

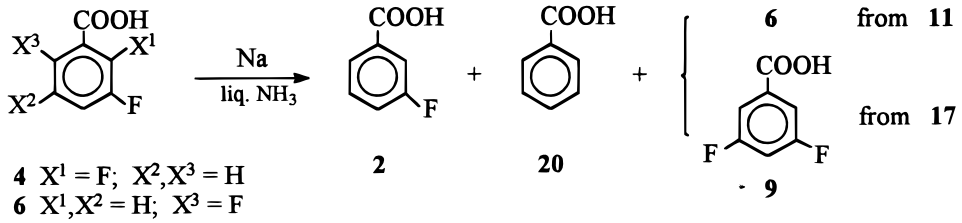

4 $X^1 = F;\ X^2, X^3 = H$
6 $X^1, X^2 = H;\ X^3 = F$
11 $X^1, X^3 = F;\ X^2 = H$
17 $X^1, X^2, X^3 = F$

SCHEME 2

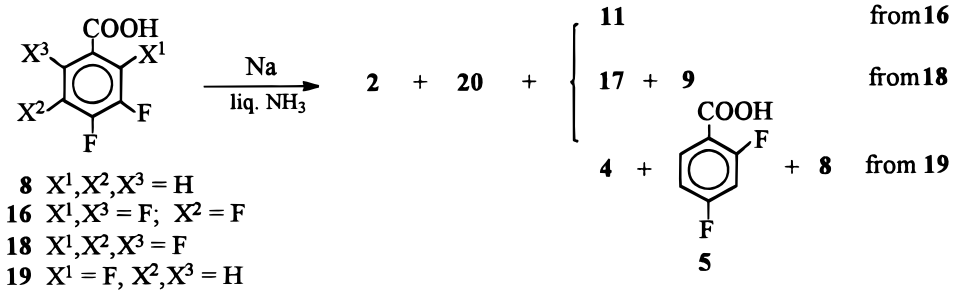

8 $X^1, X^2, X^3 = H$
16 $X^1, X^3 = F;\ X^2 = F$
18 $X^1, X^2, X^3 = F$
19 $X^1 = F,\ X^2, X^3 = H$

Regioselectivity of the Fragmentation. For polyfluorobenzoates, elimination of F^- may occur at different positions in the ring. Therefore, the k_c values to be rationalized (vide infra) must be linked to the fragmentation regioselectivity. Because of the very low concentration of the reduction products formed by EPI, their direct identification was practically impossible, and the reduction of benzoates formed by dissolving the acids **1**−**18** in liquid NH_3 and aqueous ammonium or alkali media was carried out by metals with subsequent ^1H and ^{19}F NMR product analysis.

For the treatment of acids **4**, **6**, **8**, **11, 16**−**18**, and 2,3,4-trifluorobenzoic acid (**19**) with three equivalents of alkali metals (Na, K) in liquid NH_3 (1 equiv for reaction with ammonium ion and 2 equiv for the cleavage of C−F bond) extensive defluorination of only a portion of starting material was observed with a large amount of starting compound (at times >50%) remaining unchanged to yield in all cases **2** and benzoic acid (**20**), along with other partially defluorinated acids specific for certain starting materal (Schemes 1 and 2). In general para and ortho C−F bond cleavage was predominant.

For the reduction of polyfluorobenzoates with a weaker reductant, such as Zn, there is good reason to assume the intermediate formation of RAs.[54a] The reduction of **14**, **15**, and **18** by Zn in liquid NH_3 (Scheme 3) gave only **9**, **10**, and **17**, respectively, as the products of para fluorine removal. That is, defluorination from the para position as compared to other positions is more facile. Compound **16** (Scheme 4) was converted to **11** and **12** in approximately equal amounts which suggests that the fragmentation rates of para and ortho fluorine are similar. The other fluorinated benzoates were stable under the same conditions.

To approach the conditions of the EPI experiment, the reduction of polyfluorobenzoic acids by Zn was also conducted in aqueous medium; the reaction regioselectivity remained the

SCHEME 3

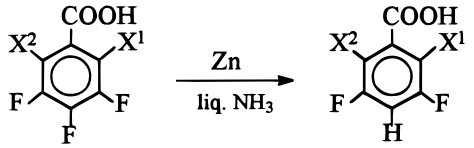

14 $X^1, X^2 = H$
15 $X^1 = F, X^2 = H$
18 $X^1, X^2 = F$

SCHEME 4

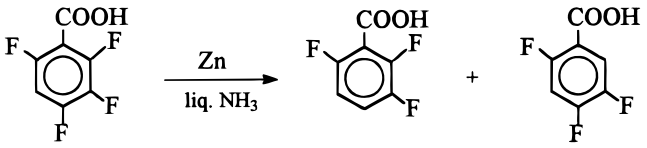

16 **11** **12**

same as in liquid NH_3. The reduction of **15** and **18** in aqueous ammonia gave only the para fluorine removal products **10** and **17**, respectively. The reduction of **18** in aqueous alkali (NaOH or KOH) gave also **17**. Thus, preference of para C−F bond cleavage was observed in both liquid NH_3 and aqueous media. The mechanism in reaction I is assumed to address the influence of various factors on the rate and the regioselectivity of RA fragmentation.[55a]

Summing up, the reduction regioselectivity of polyfluorobenzoic acids by metals in both liquid NH_3 and aqueous media correlates with the general order para > ortho > meta observed for defluorination rate constants of RAs of fluorinated benzoates in aqueous medium.

Theoretical Analysis of the RA Fragmentation. As argued in the Introduction, the fragmentation of polyfluoroarene RAs is not controlled by the $E^0_{ArX/ArX^{\bullet-}}$ and D_{ArX} thermodynamic parameters of starting ArX molecules. There is also no reason to believe that the decrease of the bond dissociation free energies of RAs, $D_{ArX^{\bullet-}}$ (the intrinsic energy barrier is related to $D_{ArX^{\bullet-}}$[2e,15d]), can be responsible for the dramatic acceleration of fragmentation with fluorine accumulation. According to the data for neutral fluoroarenes, an increase of $D_{ArX^{\bullet-}}$ with fluorine accumulation, rather than a decrease is predicted. Our semiempirical calculations for fluorobenzoate RAs, although they do not give correct absolute values, demonstrate the tendency for increasing $D_{ArX^{\bullet-}}$ values with fluorine accumulation (see also[19]). For **18** (**18′**) and **19** (**19′**) compounds, the $D_{ArX^{\bullet-}}$ of the para fluorine is predicted to be 23.95 (34.2) and 10.38 (16.09) kcal/mol, respectively, more than for **3** (**3′**) compounds. Further, for **14**, our MP2/6-31+G*//3-21+G calculations predicted the $D_{ArX^{\bullet-}}$ of the para fluorine to be 7 kcal/mol more then for **3**. The solvent reorganization energy also hardly can be responsible for the dramatic change of the RA fragmentation rate along the series of compounds under consideration, the more so they are functionally uniform. For example, the solvent reorganization energies are approximately equal for the identity electron exchange reactions of diverse benzene derivatives and their RAs.[17b]

In a general way, the specific nature of intrinsic barrier of the polyfluoroarene RAs fragmentation is directly related to the fact that fragmentation is symmetry forbidden for a planar RA. This situation is schematically illustrated in Figure 4, where Π stands for the ground π state of a RA planar structure and Σ* for its excited σ state with the SOMO localized on the breaking C−F bond.

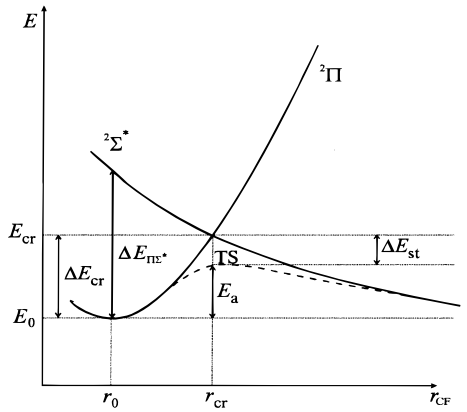

Figure 4. Schematic view of the Π and Σ* therms avoided crossing upon C−F bond stretching in the case of dissociative Σ* therm: E, total energy; r_0 and E_0, equilibrium length of the C−F bond and the total energy of starting RA, respectively; r_{cr} and E_{cr}, coordinates of the crossing point; E_a, reaction energy barrier.

TABLE 2: INDO/UHF Calculations of Low-Lying Excitations in RAs of Fluorinated Benzoates and RAs of Corresponding Benzoic Acids (Ammonium Benzoates)

	benzoates		benzoic acids (ammonium benzoates[b])		
	$\Delta E_{\Pi\Sigma^*}$ (eV)	n^a	$\Delta E_{\Pi\Sigma^*(o)}$ (eV)	$\Delta E_{\Pi\Sigma^*(m)}$ (eV)	$\Delta E_{\Pi\Sigma^*(p)}$ (eV)
1′	3.24	2	4.14 (4.22)		
2′	2.88	3		4.50 (4.58)	
3′	2.19	4			3.83 (3.96)
4′	2.68/3.11	3/2	4.01	4.16	
5′	2.19	4	3.87		3.67
6′	2.97	5	4.25	4.44	
7′			3.95		
8′	2.11	4		4.11	3.74
9′	2.99	3, 5		4.50	
10′	2.68	3	4.10	4.17/4.40	
11′	2.76	3	3.85/4.06	4.10	
12′	2.15	4	3.97	4.04	3.59
13′	2.11	4	3.65		3.47
14′	2.00	4		4.12	3.66
15′	1.99	4	3.84	3.82/4.03	3.49
16′	2.03	4	3.57/3.73	3.74	3.40
17′	2.89	3, 5	3.96	4.10	
18′	1.92	4	3.64 (3.73)	3.75 (3.97)	3.32 (3.43)
19′	2.05	4	3.75	3.80	3.56

[a] Positions of SOMO localization in Σ*(j) state. [b] Model calculations were carried out by using the optimized geometry of benzoate RA and r_{CF} = 1.363 Å. Parameters of NH_4^+ and its relative position to carboxylate group were optimized.

A C−F bond bending is necessary to avoid Π and Σ* states crossing. In the starting RA, the vibronic interaction of Π and Σ* states (pseudo-Jahn−Teller effect, PJTE), which causes the C−F bond bending, is very weak because of the significant Π−Σ* energy gap. This interaction increases dramatically as the C−F bond stretches in going to the transition state (TS) due to drastic narrowing of the Π−Σ* gap and does not exist in the products. Thus, the strong Π−Σ* vibronic interaction, which builds up with the number of fluorine substituents thus stabilizing TS, and significant out-of-plane deviation of breaking C−F bond are specific peculiarities of TS not inherent essentially in reactants and products. That is why intrinsic barrier neither stays invariant nor follows reaction free energy along the reaction series under investigation thus breaking down a parallelism of kinetics and thermodynamics.

The correlation of k_c with the reduction potential $E^0_{ArX/ArX^{\bullet-}}$ observed for monohaloarenes[2b] is due to the fact that the energy of the excited Σ* state of the corresponding RAs is practically constant with variation of the aryl moiety. Thus, the energy gap

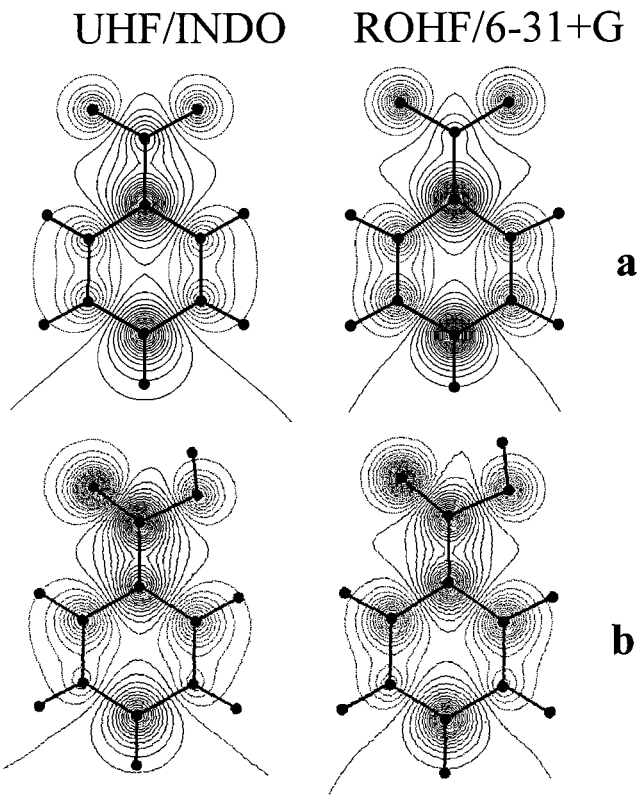

Figure 5. UHF/INDO (left) and ROHF/6-31+G (right) SOMO distribution in the ground Π state of the $C_6H_5CO_2^{\bullet 2-}$ (a) and $C_6H_5COOH^{\bullet -}$ (b).

between Π and Σ* states within the series of RAs depends only on the energy of the ground Π state. Unlike this, for polyfluoroarene RAs upon the variation of the number of fluorine atoms, the Π−Σ* gap is controlled mainly by the energy of Σ* states[19,20] (see also Table 2) thus resulting in the lack of correlation of k_c with $E^0_{ArX/ArX^{\bullet -}}$ values.

In a theoretical approach for the symmetry-forbidden fragmentation of polyfluoroarene RAs,[19,20] the location of TS is related to the Π−Σ* crossing point. The reaction energy barrier (E_a) is consistent of the crossing-point energy as the largest contribution with some corrections due to TS stabilization through out-of-plane deviation of fluorine atom and in-plane relaxation of the ring (ΔE_{st}), and the difference between solvation energies of TS and starting RA. The last term is considered constant in the series of related RAs.[19] It has been proposed that the energy gap ($\Delta E_{P\Sigma^*}$) between the Π and Σ* states of the planar structures of the starting RAs can be used as a simple reactivity index (RI).[2b] This is in fact a first approximation for the energy barrier E_a, corresponding to the relative position of the Π−Σ* crossing point with the assumption that Π state curvatures are nearly the same in the series of related RAs upon conservation of planar geometry along the coordinate corresponding to C−F bond stretching. A more rigorous approach is direct calculation of the Π and Σ* energies and modeling of the transition states.

i. Energy Gap $\Delta E_{\Pi\Sigma^*}$ as a Reactivity Index. According to UHF/INDO calculations for planar benzoate RAs an odd electron occupies the b_1-type (in terms of C_{2v} group) π-MO localized primarily in the para and ipso positions (Figure 5a). The order meta > ortho is likely due to electrostatic influence of the negatively charged CO_2^- group and is in a qualitative agreement with ab initio calculations. The lowest Σ* state is totally symmetric for all RAs, the SOMO (Figure 6) being localized mainly on the para C−Y (Y = H, F) bond (hereafter designated as Σ*(p)[56]). However, higher excited Σ* states could be involved into the PJTE as well.[57] The states responsible for fragmentation are formed by atomic orbitals making the greatest contribution to a breaking C−F bond.[58] The $\Delta E_{\Pi\Sigma^*}$ values characterizing the overall RA tendency for F^- elimination are listed in Table 2.

The $\Delta E_{\Pi\Sigma^*}$ values correctly predict the increase in the k_c values with fluorine accumulation and the preferance of para fluorine elimination. However, the predicted order ortho < meta for RAs of benzoates **1′** and **2′** disagrees with the experimentally observed k_c sequence and defluorination regioselectivity. The most probable reasons for this discrepancy are due to ignoring solvent effects and the fact that $\Delta E_{\Pi\Sigma^*}$ reflects only one, albeit the largest, contribution to the E_a value. Being nearly constant, solvation of the product species is unlikely to determine the ring position from which F^- is eliminated. In contrast, local specific (H-bond formation) and nonspecific interactions of the CO_2^- group of RA with solvent molecules or counterions may be essential. RAs of fluorinated benzoic acids can be considered as the simplest (limiting) models for such interactions of the benzoate RAs in protic solution, corresponding to complete proton transfer from solvent to the CO_2^- group. Our INDO and ab initio calculations of benzoic acid RA (Figure 5b) and of ammonium benzoate show that the ground state SOMO density is shifted from the meta to the ortho position as compared to the benzoate RA. Moreover, the $\Delta E_{P\Sigma^*}$ values for RAs of fluorinated benzoic acids exhibit excellent linear correlation (R = 0.99) with $\Delta E_{P\Sigma^*}$ for the corresponding ammonium salts (Table 2). Nonspecific solvation of benzoate RA considered in the framework of the solvaton model[49,59] gives the same result; the ratio of the coefficients associated with ortho and meta positions in b_1 π-SOMO of benzoate RA was inverted in favor of the ortho position as a natural outcome of the negative charge neutralization. For benzoic acid RAs, the Σ*(p) state was found to be the lowest, as was the case for benzoate RAs. The resulting variation of $\Delta E_{\Pi\Sigma^*}$ in the order para < ortho < meta (Table 2) agrees with the experimental data on the regioselectivity of reductive defluorination of benzoic acids. Overall, the variation of $\Delta E_{\Pi\Sigma^*}$ taken as the minimum of the $\Delta E_{\Pi\Sigma^*(j)}$ values for each RA reflects the variation of the k_c values in the series of RAs of fluorinated benzoates (Figure 7).

Thus, the model of local solvation of the CO_2^- group by its protonation results in a reasonable qualitative description of the fragmentation patterns by using $\Delta E_{\Pi\Sigma^*}$ as RI. Quantitatively, this approach underestimates the tendency of F^- elimination from the ortho position in the RA.

ii. Calculations of a Reaction Path and Modeling of the Transition States. As stated above, the solvation of F^- makes the Σ* state of the RA C−F bond scission dissociative. In a gas phase, the energy of the Σ* state increases monotonically leading to the reaction products plateau.[19,20] To model the TS we calculated the potential energy curves of C−F bond stretching for Π and Σ* states and located their crossing-point position. For each RA we considered the F^- elimination corresponding to the lowest $\Delta E_{\Pi\Sigma^*(j)}$ value.

According to the calculations, the SOMO of the ground Π state changes insignificantly, remaining the b_1-type MO up to the crossing point. Unlike that, the SOMO of the Σ* state localizes on the breaking C−F bond along the reaction coordinate, i.e., upon ortho or meta F^- elimination the Σ*(p) state changes to Σ*(o) and Σ*(m), respectively. With para C−F bond cleavage in the vicinity of Π−Σ* crossing the initial SOMO localizations in the Π and Σ*(p) states coincide and thus provide efficient vibronic interaction. The structure obtained

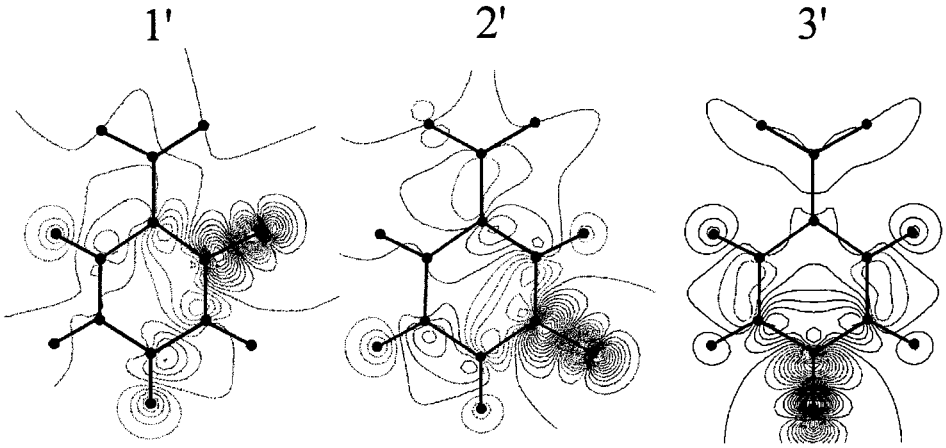

Figure 6. SOMO plots (UHF/INDO) for the lowest excited Σ*(*j*) states of **1′**−**3′** monofluorobenzoate RAs.

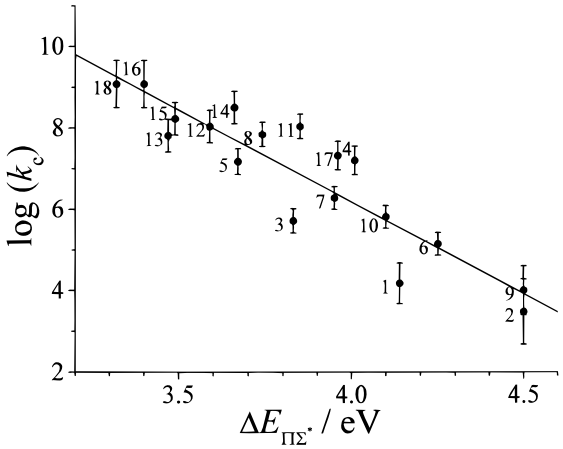

Figure 7. Relationship between the $\Delta E_{\Pi\Sigma^*}$ values calculated for RAs of fluorinated benzoic acids and the experimental fragmentation rate constants k_c of the RAs of corresponding benzoates; $R = 0.91$.

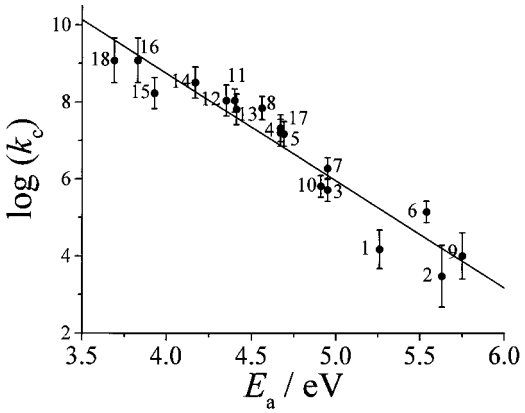

Figure 8. Relationship between the model reaction energy barrier E_a for the fragmentation of F^- from the RAs of fluorobenzoic acids and the experimental fragmentation rate constant k_c of the RAs of corresponding benzoates; $R = 0.96$.

at the C−F distance $r_{CF} = r_{cr}$ by optimization of all other geometrical parameters[19] was assumed to be a good model of the TS stabilized by the out-of-plane deviation of the leaving fluorine atom due to vibronic interaction of the Π and Σ*(p) states. A different situation obtains for F^- elimination from the ortho or meta positions. The vibronic interactions are not efficient in the vicinity of crossing by virtue of different spatial SOMO localizations in Π and Σ*(o) or Σ*(m) states. In these cases stabilization of the TS can result from the interaction between the Σ*(*j*) and Π* states since the SOMO of the latter, which is an a_2-type MO, is localized at the ortho and meta positions. We therefore simulated the TS for ortho and meta C−F bond cleavage using the structures obtained by optimization with the distance $r_{CF} = r_\theta$, where r_θ corresponds to the "crossing"[60] of the potential curves of C−F bond stretching in the plane of the ring and with optimum for each r_{CF} deviation from this plane.

As with the $\Delta E_{\Pi\Sigma^*}$ approach, TS modeling for benzoate RAs failed to describe the experimental k_c values. In contrast, similar calculations for RAs of the corresponding benzoic acids as models of solvated benzoate RAs resulted in satisfactory linear correlation between the E_a and log k_c values (Figure 8).

Thus, the rationalization of experimental rate constants of RA fragmentation in the series of fluorinated benzoates requires taking into account both local solvation of the CO_2^- group and TS stabilization due to out-of-plane distortions. The calculations show that the TS of F^- elimination from RAs of fluoroaromatic compounds is essentially nonplanar.

Conclusion

The fragmentation rate constants, k_c, for RAs of polyfluorinated benzoates in aqueous solutions (pH 13.4) show an increase of about 6 orders of magnitude with fluorine atom accumulation depending on the orientation of the fluorine atoms in the aromatic ring. The rate of F^- elimination depends on its orientation with respect to the CO_2^- group in the order para > ortho > meta. The mutual orientation of fluorine atoms has a significant effect; specifically, k_c values sharply increase when adjacent fluorine atoms are present. For adequate interpretation of the regio dependence of k_c values, both local solvation of the CO_2^- group and TS stabilization by out-of-plane distortion must be considered. The model energy barriers of fragmentation, estimated for RAs of fluorinated benzoic acid from INDO/UHF calculations, give a good linear relationship ($R = 0.96$) with the experimental log k_c values, accounting for both fluorine accumulation and isomer effects.

Acknowledgment. This work was partially supported by the Russian Foundation of Basic Research under Grants 96-03-32984a, 99-03-33111a (S.S.L. and V.D.S.) and 97-03-33667a (I.V.B. and L.N.S.). The authors are grateful to the late Prof. P. V. Shchastnev who stimulated us with regard to the quantum mechanical calculations.

References and Notes

(1) (a) Behar, D.; Neta, P. *J. Am. Chem. Soc.* **1980**, *102*, 4798. (b) Neta, P.; Behar, D. *J. Am. Chem. Soc.* **1981**, *103*, 103. (c) Behar, D.; Neta, P. *J. Am. Chem. Soc.* **1981**, *103*, 2280.

(2) (a) Andrieux, C. P.; Blocman, C.; Dumas-Bouchiat, J.-M.; M'Halla, F.; Savéant, J.-M. *J. Am. Chem. Soc.* **1980**, *102*, 3806. (b) Andrieux, C. P.; Savéant, J.-M.; Zann, D. *Nouv. J. Chim.* **1984**, *8*, 107.

(3) (a) Bunnett, J. F. *Acc. Chem. Res.* **1978**, *11*, 413. (b) Rossi, R. A.; de Rossi, R. M. *Aromatic Substitution by the $S_{RN}1$ Mechanism*; American Chemical Society: Washington, DC, 1983. (c) Savéant, J.-M. *Acc. Chem. Res.* **1980**, *13*, 323. (d) Savéant, J.-M. *Adv. Phys. Org. Chem.* **1990**, *26*, 1. (e) Savéant, J.-M. *Tetrahedron* **1994**, *50*, 10117. (f) Shteingarts, V. D.; Kobrina, L. S.; Bilkis, I. I.; Starichenko, V. F. *Chemistry of Polyfluoroarenes: Mechanism of Reactions, Intermediates*; Nauka: Novosibirsk, 1991 (in Russian). (g) Todres, Z. V. *Radical Ions in Organic Synthesis*; Khimiya: Moscow, 1986 (in Russian). (h) Mendkovich, A. S.; Gultjai, V. P. *Theoretical Aspects of Chemistry of Organic Radical Anions*; Nauka: Moscow, 1990 (in Russian).

(4) (a) Konovalov, V. V.; Raitsimring, A. M.; Tsvetkov, Yu. D.; Bilkis, I. I. *Chem. Phys. Lett.* **1989**, *157*, 257. (b) Konovalov, V. V.; Tsvetkov, Yu. D.; Bilkis, I. I.; Laev, S. S.; Shteingarts, V. D. *Mendeleev Commun.* **1993**, 51.

(5) (a) Shchegoleva, L. N.; Bilkis, I. I.; Schastnev, P. V. *Chem. Phys.* **1983**, *82*, 343. (b) Starichenko, V. F.; Shchegoleva, L. N.; Efremova, N. V.; Shteingarts, V. D.; Saik, V. O.; Schastnev, P. V. *Chem. Phys.* **1985**, *100*, 79. (c) Lozovoy, V. V.; Grigoryants, V. M.; Anisimov, O. A.; Molin, Yu. N.; Schastnev, P. V.; Shchegoleva, L. N.; Bilkis, I. I.; Shteingarts, V. D. *Chem. Phys.* **1987**, *112*, 463.

(6) (a) Anbar, M. *Adv. Phys. Org. Chem.* **1969**, *7*, 115. (b) Freeman, P. K.; Srinivasa, R. *J. Org. Chem.* **1987**, *52*, 252.

(7) Clarke, D. D.; Coulson, C. A. *J. Chem. Soc. A* **1969**, *2*, 169.

(8) Parker, V. D. *Adv. Phys. Org. Chem.* **1983**, *19*, 132.

(9) (a) Andrieux, C. P.; Savéant, J.-M. Electrochemical Reactions. In *Investigation of Rates and Mechanisms of Reactions, Techniques of Chemistry*; Bernasconi, C. F., Ed.; Wiley: NewYork, 1986; Vol. VI/4E, Part 2, p 305. (b) Andrieux, C. P.; Hapiot, P.; Savéant, J.-M. *Chem. Rev.* **1990**, *90*, 723.

(10) Andrieux, C. P.; Savéant, J.-M.; Tallec, A.; Tardivel, R.; Tardy, C. *J. Am. Chem. Soc.* **1996**, *118*, 9788.

(11) (a) Andersen, M. L.; Mathivanan, N.; Wayner, D. D. M. *J. Am. Chem. Soc.* **1996**, *118*, 4871. (b) Andersen, M. L.; Lang, W.; Wayner, D. D. M. *J. Am. Chem. Soc.* **1997**, *119*, 6590. (c) Antonello, S.; Musumeci, M.; Wayner, D. D. M. *J. Am. Chem. Soc.* **1997**, *119*, 9541.

(12) For a review, see ref 4e.

(13) Andrieux, C. P.; Combellas, C.; Kanoufi, F.; Savéant, J.-M.; Thiébault, C. *J. Am. Chem. Soc.* **1997**, *119*, 9727.

(14) Efremova, N. V.; Starichenko, V. F.; Shteingarts, V. D. *Zh. Org. Khim.* **1988**, *24*, 57.

(15) (a) Amatore, C.; Combellas, C.; Pinson, J.; Oturan, M. A.; Robveille, S.; Saveant, J.-M.; Thiebault, A. *J. Am. Chem. Soc.* **1985**, *107*, 4846. (b) Andrieux, C. P.; Saveant, J.-M.; Su, K. B. *J. Phys. Chem.* **1986**, *90*, 3815. (c) Savéant, J.-M. *J. Am. Chem. Soc.* **1987**, *109*, 6788. (d) Saveant, J.-M. *J. Phys. Chem.* **1994**, *98*, 3716.

(16) The driving force of the reaction I (where we neglect the entropies) is[15d] $\Delta G^{o} = E^{-0}_{\mathrm{ArX/ArX}^{\bullet}} - E^{0}_{\mathrm{ArX/Ar}^{\bullet}+\mathrm{X}^{-}} = D_{\mathrm{ArX}} + E^{0}_{\mathrm{ArX/ArX}^{\bullet-}} - E^{0}_{\mathrm{X}^{\bullet}/\mathrm{X}^{-}}$; D_{ArX} is the bond dissociation energy into $\mathrm{Ar}^{\bullet}$ and $\mathrm{X}^{\bullet}$.

(17) (a) Steppard, W. A.; Sharts, C. M. *Organic Fluorine Chemistry*; W. A. Benjamin, Inc.: New York, 1969. (b) Eberson, L. *Adv. Phys. Org. Chem.* **1982**, *18*, 79.

(18) Fenzlaff, M.; Illenberger, E. *Chem. Phys.* **1989**, *136*, 443.

(19) Shchegoleva, L. N.; Schastnev, P. V. *Zh. Fiz. Khim.* **1991**, *65*, 1789.

(20) Schastnev, P. V.; Shchegoleva, L. N. *Molecular Distortions in Ionic and Excited States*; CRC Press: Boca Raton, 1995.

(21) In a pulse radiolysis experiment, the range of k_c determination is limited by the necessity of separating e^{-}_{aq} and RA spectra and the low solubility of organic compounds.

(22) (a) Barker, G. C.; Gardner, A. W.; Sammon, D. C. *J. Electrochem. Soc.* **1966,** *113*, 1182. (b) Pleskov, Yu. V.; Rotenberg, Z. A.; Eletsky, V. V.; Lakomov, V. I. *Discuss. Faraday Soc.* **1974**, *56*, 52. (c) Gurevich, Yu. Ya.; Pleskov, Yu. V.; Rotenberg, Z. A. *Photoelectrochemistry*; Plenum Press: New York, 1980. (d) Benderskii, V. A.; Krivenko, A. G. *Usp. Khim.* **1990**, *59*, 3. (Engl transl: *Russian Chem. Rev.* **1990**, *59*, 1.). (e) Benderskii, V. A.; Benderskii, A. A. *Laser Electrochemistry of Intermediates*; CRC Press: Boca Raton, 1995.

(23) (a) Konovalov, V. V.; Tregub, V. V.; Raitsimring, A. M. *Electrokhimia* **1984**, *20*, 470. (b) Konovalov, V. V.; Raitsimring, A. M.; Tsvetkov, Yu. D.; Benderskii, V. A. *Chem. Phys.* **1985**, *93*, 163. (c) Konovalov, V. V.; Raitsimring, A. M.; Tsvetkov, Yu. D. *J. Electroanal. Chem.* **1990**, *292*, 33.

(24) (a) Konovalov, V. V.; Raitsimring, A. M.; Tsvetkov, Yu. D. *Radiat. Phys. Chem.* **1988**, *32*, 623. (b) Konovalov, V. V.; Raitsimring, A. M. *Chem. Phys. Lett.* **1990**, *171*, 326. (c) Kalugin, A. I.; Konovalov, V. V.; Shokhirev, N. V.; Raitsimring, A. M. *J. Electroanal. Chem.* **1993**, *359*, 63. (d) Kalugin, A. I.; Konovalov, V. V.; Raitsimring, A. M. *J. Electroanal. Chem.* **1993**, *362*, 185.

(25) Konovalov, V. V.; Bilkis, I. I.; Selivanov, B. A.; Shteingarts, V. D.; Tsvetkov, Yu. D. *J. Chem. Soc., Perkin Trans. 2* **1993**, 1707.

(26) (a) Hapiot, P.; Konovalov, V. V.; Savéant, J.-M. *J. Am. Chem. Soc.* **1995**, *117*, 1428. (b) Gonzales, J.; Hapiot, P.; Konovalov, V. V.; Savéant, J.-M. *J. Am. Chem. Soc.* **1998**, *120*, 10171.

(27) (a) The most positive electrode potential E for EPI measurements is determined by the photoinjection threshold potential E_{thr}. At the wavelength 351 nm for aqueous 0.5 M KCl and mercury electrode, $E_{\mathrm{thr}} = 0.14$ V (SCE).[23c] The most negative potential is determined by the electrochemical reduction of the solution species.[27b,c] (b) The electrode potential for hydrogen evolution in aqueous solutions at mercury electrode is about -2.0 V (SCE). (c) Half-wave potentials of **18** in 75% dioxane/water solution are -1.74 V (SCE) (COOH group reduction) and -2.49 V (benzene ring reduction),[27d] and those of benzoic acid **20** are -1.94 V and -2.46 V, respectively.[27e] (d) Bartle, W. W.; Eggins, B. R. *J. Polarog. Soc.* **1966**, *12*, 89. (e) von Stackelberg, M.; Stracke, W. *Z. Electrochem.* **1949**, *53*, 118.

(28) (a) Standard potential of e^{-}_{aq} is -2.85 V (SCE).[33b] (b) Swallow, A. J. *Radiation Chemistry*; Longman: London, 1973; p 148.

(29) (a) The INDO-optimized geometry of the hexafluorobenzene RA[20] is in good agreement with the results of ROHF/6-31+G* calculations.[29b] In contrast, MNDO, AM1, and PM3 methods do not give correct descriptions of the polyfluorobenzene RA structure and spin density distribution.[29c] (b) Shchegoleva, L. N.; Beregovaya, I. V.; Schastnev, P. V. *Magn. Resonan.and Relat. Phenom.* (Vol. II, Proc. Joint 29th AMPER–13th ISMAR Conference, Berlin) **1998**, 889. (c) Shchegoleva, L. N.; Bliznyuk, A. A. Unpublished results.

(30) Preliminary data on the fragmentation rate constants of polyfluorinated benzoate RAs have been published in a short communication.[4b] However, the k_c values had not been determined for all polyfluorinated benzoates, the problem connecting the rates and the regioselectivity of RAs fragmentation remained unsolved, and the fragmentation trends had not been rationalized.

(31) Melting points were determined with a Kofler apparatus and are uncorrected.

(32) *Aldrich 1998–1999, Catalog Handbook of Fine Chemicals*; Aldrich Chemical Co.: Milwaukee, 1998.

(33) Holland, D. G.; Moore, G. J.; Tamborski, C. *J. Org. Chem.* **1964**, *29*, 3042.

(34) Tamborski, C.; Soloski, E. J. *J. Org. Chem.* **1966**, *31*, 746.

(35) Deacon, G. B.; Phillips, R. J. *Aust. J. Chem.* **1978**, *31*, 1709.

(36) Bergmann, E. D.; Bercovic, S. *J. Org. Chem.* **1961**, *26*, 919.

(37) Minor, J. T.; Vanderwerf, C. A. *J. Org. Chem.* **1952**, *17*, 1425.

(38) Shtark, A. A.; Chuikova, T. V.; Selivanova, G. A.; Shteingarts, V. D. *Zh. Org. Khim.* **1987**, *23*, 2574.

(39) Roe, A.; Little, W. F. *J. Org. Chem.* **1955**, *20*, 1577.

(40) Pozdnyakovich, Yu. V.; Shteingarts, V. D. *J. Fluorine Chem.* **1974**, *4*, 317.

(41) Finger, G. C.; Gortatowski, M. J.; Shiley, R. H.; White, R. H. *J. Am. Chem. Soc.* **1959**, *81*, 94.

(42) Yakobson, G. G.; Odinokov, V. N.; Vorozhtsov, N. N. *Zh. Obshchei Khim.* **1966**, *36*, 139.

(43) Laev, S. S.; Shteingarts, V. D.; Bilkis, I. I. *Tetrahedron Lett.* **1995**, *36*, 4655.

(44) Kobrina, L. S.; Yakobson, G. G. *Zh. Obshchei Khim.* **1965**, *35*, 2055.

(45) Laev, S. S.; Shteingarts, V. D. *Tetrahedron Lett.* **1997**, *38*, 3765.

(46) Schmidt, M. W.; Baldridge, K. K.; Boatz, J. A.; Elbert, S. T.; Gordon, M. S.; Jensen, J. H.; Koseki, S.; Matsunaga, N.; Nguyen, K. A.; Su, S. J.; Windus, T. L.; Dupuis, M.; Montgomery, J. A. *J. Comput. Chem.* **1993**, *14*, 1347.

(47) Plakhutin, B. N. *SFQP-23, Informational Materials of a Specialized Fund of Quantum Chemical Programs (SFQP) of Siberian Branch of the Academy of Sciences of USSR*; Institute of Chemical Kinetics and Combustion: Novosibirsk, 1989; Vol. 3, p 16 (in Russian).

(48) Gorb, L. G.; Abronin, I. A. *SFQP-49* **1989**, *3*, 22 (in Russian).

(49) Schaftenaar, G. *QCPE-619*.

(50) (a) RA of benzoate (**20′**) in aqueous solution has $pK_{BH^+} = 12$ for protonation at CO_2^-.[50b] For RAs of fluorinated benzoates, pK_{BH^+} is expected to decrease with fluorine atom accumulation. For the basicity of ring position occupied by fluorine, the value $pK_{BH^+} = 12.4$, estimated for the hexafluorobenzene RA,[50c] can be assumed as typical. (b) Simic, M.; Hoffman, M. Z. *J. Phys. Chem.* **1972**, *76*, 1398. (c) Shoute, L. C. T.; Mittal, J. P. *J. Phys. Chem.* **1993**, *97*, 379.

(51) Compton, R. G.; Harding, M. S.; Pluck, M. R.; Atherton, J. H.; Brennan, C. V. *J. Phys. Chem.* **1993**, *97*, 10416.

(52) Hart, E. J.; Anbar, M. *Hydrated electron*; Wiley: New York, 1970.

(53) Konovalov, V. V.; Bilkis, I. I.; Laev, S. S.; Raitsimring, A. M. In *Proceeding of 5th Working Meeting on Radiation Interaction*; Leipzig, 1990; p 204.

(54) (a) The generation of RAs was observed directly from nonhalogenated arenes in system the Zn/OH^-–DMSO[54b] and from hypericin in the systems Zn/DMF or Zn/DMF–H_2O.[54c] The formation and cleavage of RAs were proposed in the defluorination of perfluoroolefins by Zn/DMF[54d] and perfluoroarenes by Zn/Cu in DMF–H_2O.[54e] (b) Kishan, L. H.; Kanchan,

G. *Tetrahedron Lett.* **1986**, *27*, 1371. (c) Gerson, F.; Gescheidt, G.; Haring, P.; Mazur, Y.; Freeman, D.; Spreitzer, H.; Daub, J. *J. Am. Chem. Soc.* **1995**, *117*, 11861. (d) Hu, Ch.-M.; Long, F.; Xu, Ze-Qi *J. Fluorine Chem.* **1990**, *48*, 29. (e) Krasnov, V. I.; Platonov, V. E. *Zh. Org. Khim.* **1993**, *29*, 1078.

(55) (a) As an alternative to direct RA fragmentation, protonation of RA at the ipso position to a fluorine atom, followed by reduction of the resulting radical and subsequent removal of F^- should be considered.[55b] However, for RAs of monohalobenzoic acids (X = F, Cl, Br) this mechanism has been ruled out[4a] since the k_c values were found to be independent of pH within the range 4−13. Moreover, the k_c values for the majority of polyfluorinated benzoate RAs exceed the pseudo-first-order rate constant of protonation of RA at the ring positions which can be estimated as $\sim 10^6$ s^{-1}.[50b,55c] (b) Mishra, S. P.; Symons, M. C. R. *J. Chem. Soc., Perkin Trans. 2* **1981**, 185. (c) Dorfman, L. M. *Acc. Chem. Res.* **1970**, *3*, 224.

(56) Here and later, an index in parentheses designates the position of primary SOMO localization.

(57) Bersuker, I. B.; Gorinchoi, N. N.; Polinger, V. Z. *Multielectron Problem in Quantum Chemistry*; Kiev: Nauk. Dumka, 1987 (in Russian).

(58) These states are of the same symmetry as the lower Σ*(p) state, which generally makes their direct calculation impossible within the framework of the Hartree−Fock (HF) approximation. Nevertheless, due to the distinction between spatial SOMO localization in different Σ*(*j*) states (up to 75% of the unpaired electron density is concentrated on the C−F bond in the *j*th position) in some cases (Table 2) it is possible to obtain self-consistent field HF solutions corresponding to the individual Σ*(*j*) states (see also Experimental section).

(59) Gorb, L. G.; Abronin, I. A.; Khartchevnikova, N. V.; Zhidomirov, G. M. *Zh. Fiz. Khim.* **1984**, *58*, 9.

(60) There is no real crossing since the potential curves relate to different geometric structures. We mean a coincidence of the total energies of these structures at the r_{CF} value.